The interaction of oil and lipids in freestanding lipid bilayer membranes studied with label-free high-throughput wide field second harmonic microscopy

Orly B. Tarun[1], Maksim Yu. Eremchev[1] and Sylvie Roke*[1]

[1]*Laboratory for fundamental BioPhotonics (LBP), Institute of Bioengineering (IBI), and Institute of Materials Science (IMX), School of Engineering (STI), and Lausanne Centre for Ultrafast Science (LACUS), École Polytechnique Fédérale de Lausanne (EPFL), CH-1015 Lausanne, Switzerland*

**Corresponding author: sylvie.roke@epfl.ch*

Abstract The interaction of oils and lipids is relevant for membrane biochemistry since the cell uses bilayer membranes, lipid droplets and oily substances in its metabolic cycle. In addition, a variety of model lipid membrane systems, such as freestanding horizontal membranes and droplet interface bilayers are made using oil to facilitate membrane monolayer apposition. We characterize the behavior of excess oil inside horizontal freestanding lipid bilayers using different oils, focusing on hexadecane and squalene. Using a combination of second harmonic (SH) and white-light imaging, we measure how oil redistributes within the membrane bilayer after formation. SH imaging shows that squalene forms a wider annulus compared to hexadecane suggesting that there is a higher quantity of squalene remaining in the bilayer compared to hexadecane. Excess oil droplets that appear right after membrane formation are tracked with white-light microscopy. Hexadecane droplets move directionally to the edge of the membrane with diffusion constants similar to single lipids, while squalene oil droplets move randomly with lower diffusion speeds similar to lipid condensed domains and remain trapped in the center of the bilayer for ~1-3 hours. We discuss the observed differences in terms of different coupling mechanism between the oil and lipid molecules induced by the different chemical structures of the oils.

Introduction

The lipid bilayer membrane that surrounds cells and organelles performs a wide variety of functions ranging from regulating transport, to signaling and providing a protective barrier. As such membranes come in contact with many substances, for example with lipid droplets. Lipid droplets are composed of an oil-based core covered with a monolayer of lipids and proteins, that serve as energy storage and play a fundamental role in cell metabolism.[1] These lipid droplets can merge with cell membranes and deposit their oily core within the bilayer.[2] It can therefore be expected that lipid membranes can at times contain hydrophobic molecules. In addition, oily substances within the bilayer are relevant for a variety of membrane processes. For example, some proteins require a thicker hydrophobic core (such as perilipins or alcoholdehydrogenases) to function optimally,[3-6] trans-membrane motion (flip-flop), membrane diffusion and raft formation require membrane reorganization[7-8] that is influenced by oil. Thus, the interactions of oily substances with lipids are relevant for biological processes. However, there is no molecular level information about the interactions of oil and lipids in real cells or even in free standing model membrane systems that are recognized to capture essential membrane biophysics/chemistry.[9] While many model membrane studies[10-16] focus on the phase behavior of lipids,[8, 17-18] or lipids and steroids[19-21] not much work has been dedicated to the interaction of hydrophobic oils and lipids. In addition, oils are needed to prepare the membrane system, such as in the case of freestanding lipid bilayers[15-16] and droplet interface bilayers (DIBs).[22] From this point of view, it is of interest to understand better how oils and lipids interact and what this interaction means for the properties of the membrane.

Here we study the interaction of oil with freestanding lipid bilayer membranes using white light and label-free non-resonant second harmonic imaging. The freestanding bilayers are formed in a ~100 micron wide and ~25 micron thick aperture in a Teflon film that is pre-painted with an oil mixture. This oil serves as a transition material between the Teflon edge (25 microns thick) and the lipid membrane (~ 6 nm thick).[16] Fig. 1A shows a top view image of the Teflon ring with a membrane in the center of the aperture. At the perimeter of the bilayer region there is a transition region that contains oil. This region can be seen as an annulus in the wide field image of Fig. 1A and contains a volume of oil that is located between the edge of the aperture and the lipid bilayer, sketched as a side view in Fig. 1A. We determine how oil redistributes within the bilayer after membrane formation and assess whether oil remains between or within opposing leaflets or leaves the bilayer region after equilibration. We vary the structure of the oil studying saturated alkanes (hexadecane and heptadecane) and a branched oil structure (squalene), Fig. 1B. We observe differences in the interaction of both types of oils with the membrane system. Hexadecane droplets are

seen to move directionally to the edge of the membrane with diffusion constants similar to that of single lipids. Squalene oil droplets move randomly with lower diffusion speeds similar to lipid condensed domains and remain trapped in the center of the bilayer for ~1-3 hours. We discuss the observed differences in terms of different coupling mechanism between the oil and lipid molecules induced by the different chemical structures of the oils.

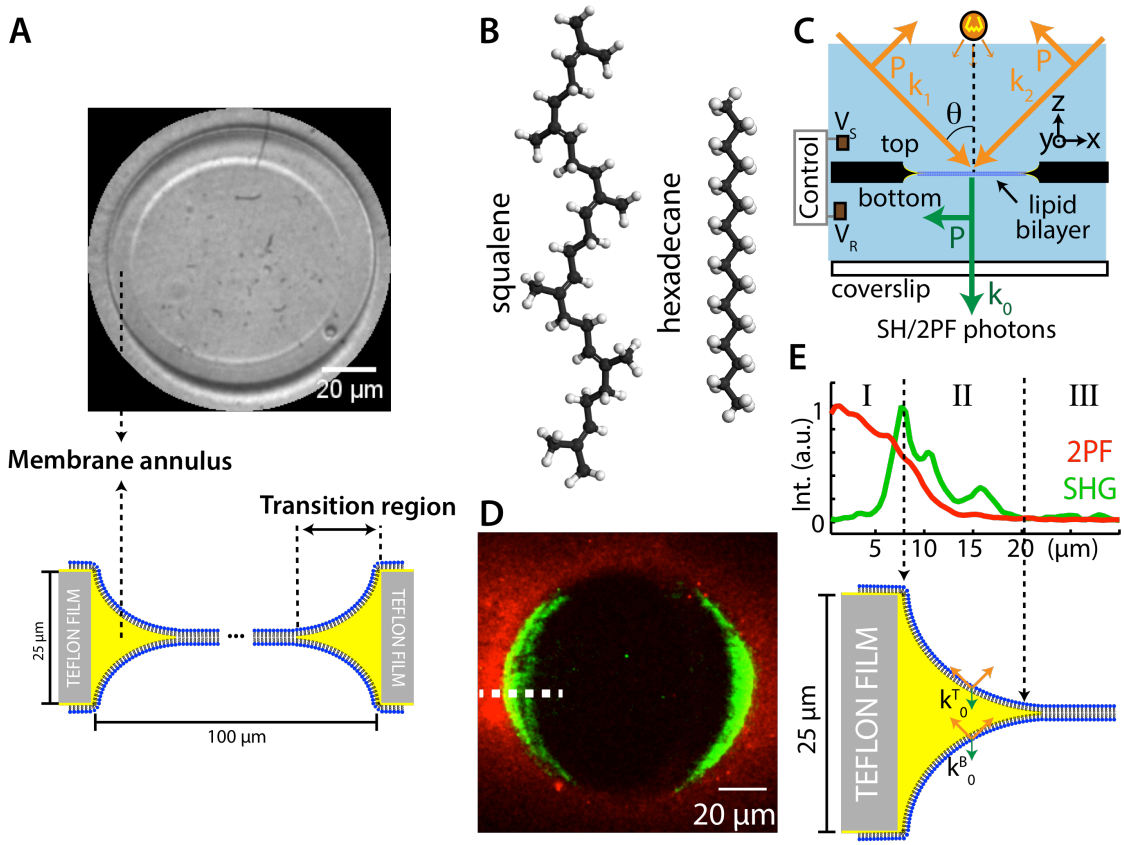

Figure 1. Second harmonic (SH) imaging of freestanding lipid bilayers. **(A)** While light image (top) and schematic (bottom, drawn not to scale) of a freestanding DOPC lipid bilayer with a wide oil (squalene) annulus at the periphery of the membrane. **(B)** Illustrations of the alkanes used in this study. (**C**) Schematic of the imaging setup with counter propagating beams that overlap in space and time to illuminate the membrane (blue). The second harmonic (SH) photons and two-photon fluorescence (2PF) are collected in the phase-matched direction. Abbreviations: P – plane of incidence, $k_{1/2}$ – wave vector of the excitation beams, k_0 – wave vector of the emitted beam, V_S – signal electrode, V_R – reference electrode. **(D)** SH (green) and two-photon fluorescence (red) images of a symmetric neutral membrane composed of DOPC. (**E**) Line profiles (10 pixels wide) of the dashed lines in D with the vertical cross-section (x-z plane in C) of the sample showing the structure of the Teflon film (gray, region I), oil (yellow) and monolayer leaflets (blue) (region II) thinning to form a lipid bilayer in the aperture center (region III). k^T_0 and k^B_0 correspond to the second harmonic photons generated from the top and bottom bilayer leaflets respectively.

Experimental Section

Chemicals 1,2-dioleoyl-sn-glycero-3-phosphocholine (DOPC), 1,2-diphytanoyl-sn-glycero-3-phosphocholine (DPhPC), hexadecane ($C_{16}H_{34}$, 99.8%, Sigma-Aldrich), squalene ($C_{30}H_{50}$, >98%, Sigma-Aldrich), heptadecane ($C_{17}H_{36}$, 99.5%, Sigma-Aldrich), hexane (C_6H_{14}, Sigma-Aldrich, >99%), chloroform (Merck, >99.8%), hydrogen peroxide (30%, Reactolab SA), sulfuric acid (95-97%, ISO, Merck), KCl (99.999%, Aros) were used as received. All aqueous solutions were made with ultra-pure water (H_2O, Milli-Q UF plus, Millipore, Inc., electrical resistance of 18.2 MW cm). All aqueous solutions were filtered with 0.1 μM Millex filters. The coverslips used in the imaging were pre-cleaned with piranha solution (1:3 - 30% H_2O_2: 95-97% H_2SO_4) and thoroughly rinsed with ultrapure water.

Sample preparation A freestanding horizontal planar lipid bilayer is formed in a 80-120 μm sized circular aperture in a 25 μm thick Teflon film by apposition of two separated lipid monolayers[16, 23] that are formed at two separate air/water interfaces. For more information on sample preparation see the supplementary information (SI, S1)

Imaging experiments The SH imaging setup has been previously characterized in detail, see Refs.[24-26]. In brief, two counter propagating beams (pulse duration of 190 fs, wavelength of 1030 nm and repetition rate of 200 KHz from a Yb:KGW femtosecond laser, (Light Conversion Ltd.)) were incident at 45° with respect to the surface normal (see fig. 1C). The beams were loosely focused using a f=20 cm doublet lens (B coating, Thorlabs). The phase-matched SH photons were collected with a 50x objective lens (Mitutoyo Plan Apo NIR HR Infinity-Corrected Objective, 0.65 NA in combination with a tube lens (Mitutoyo MT-L), a 900 nm short pass filter (FES0900, Thorlabs), a 515 nm band pass filter (FL514.5-10) and an intensified electronically amplified CCD camera (IE-CCD, PiMax4, Princeton Instruments). A 400 mm meniscus lens was placed behind the objective lens to remove spherical aberrations induced by the coverslip. The transverse resolution was 430 nm. All images were recorded with the beams polarized parallel to the plane of incidence (P). Fluorescence measurements were performed with the same imaging setup. A 550 nm long pass filter (FEL0550, Thorlabs) was placed before the detector to detect the outgoing two-photon fluorescence. For white-light imaging, the sample is illuminated from the top using a white light source and the linear scattered light is detected in the forward direction with the same objective lens. (Fig. 1C).

Results and Discussion

SH and white-light imaging of freestanding horizontal bilayers.

Capacitance measurements of freestanding membranes[27-29] have been performed for bilayers prepared with various oils. These studies suggest that the apposition of two lipid monolayers drives the oil to the edges of the bilayer (into the transition region that we term the annulus).[30] Since capacitance is inversely proportional to thickness, high-capacitance membranes are interpreted as thin membranes and the calculated thickness that is measured matches the thickness of the hydrophobic core of a bilayer, thus suggesting that freestanding bilayers are solvent-free for squalene and hexadecane.[16, 27] Later studies performed with oils that have varying alkane chain lengths showed that bilayers prepared with short chain alkanes have a lower capacitance suggesting that shorter chain alkanes have the tendency to stay in the middle of the bilayer.[12, 15, 28-29] In this study, we investigate these findings more deeply and focus on the behavior of hexadecane and squalene. Figure 1D shows a SH image (SHG, green) and two-photon fluorescence (2PF, red) of a symmetric neutral membrane composed of 1,2-dioleoyl-sn-glycero-3-phosphocholine (DOPC). The images are collected with all beams polarized in the P direction (with the electric field oscillating in the plane of the wave vectors of the beams). The line profiles (10 pixels wide) marked by the dashed lines in Fig. 1D are shown in Fig. 1E. The 2PF intensity decreases from the edge (red) while the SH signal vanishes in the center and increases towards the edge while displaying oscillations. The 2PF arises from the Teflon film and decays smoothly. This decay arises from the shape of the aperture, as the opening in the Teflon film is tapered and not cylindrical. In terms of structure, going from the edge (region I) of the Teflon film towards the center, there is a transition region composed of an oil phase bordered by a lipid / water interface. This transition region (region II) thins towards the center of the lipid film (region III). The central part of the symmetric bilayer (region III) generates no SH photons (green line profile) because within the dipole approximation,[31] oppositely oriented polar molecules in and around the symmetric bilayer interfere destructively (emitting SH light with a phase difference of π) and do not emit SH photons. This also suggests that there are no oil molecules detected from the center since as little as a monolayer of oil would lead to breaking of centrosymmetry. However, the transition region at the edge (region II) generates SH photons. The intensity increases towards the edge, coinciding with an increasing distance between the monolayer leaflets. The reason for the SH generation is that the symmetry of the (symmetric) bilayer is gradually broken, as the SH photons (k^T_0 and k^B_0 from the top and bottom leaflets) are emitted with phases that deviate from π, such that the interference becomes more constructive towards the edge of the film. The coherence length, defined as $l_c = \pi \Delta k_z{}^{-1}$ where Δk_z the wave vector mismatch, is given by $\Delta k_z = |\boldsymbol{k}_{1z} +$

$\boldsymbol{k}_{2z}-\boldsymbol{k}_{0z}| = k_{1z} + k_{2z}-k_{0z}$, with $\boldsymbol{k}_{1,2}$ the incoming wave vectors and $\boldsymbol{k}_0$ the outgoing wave vector. In our experiment, the phase matching distance is 386.5 nm and the corresponding coherence length l_c is 1.2 μm. As the leaflets curve toward the Teflon edge, the SH intensity displays minima and maxima that arise from phase changes dependent on the distance between leaflets. In addition to this beating, as the monolayer leaflets curve, the orientation of the interface changes relative to the polarization direction of the incoming electric fields such that the interface and the polarization become more parallel. This process ensures that the SH intensity displays an overall increase. The combined effect results in the pattern displayed by the green curve in Fig. 1E.

The intensity distribution of the SH images is thus sensitive to the distance between the leaflets, and the SH intensity distribution of a symmetric bilayer can be used to estimate the presence of oil in the bilayer. The width of region II in Fig. 1D quantifies the width of the annulus and the amount oil in the bilayer. We can thus use this property to investigate the interaction of squalene and hexadecane with the lipid bilayer. If the annulus is wide, it means the oil mixes more easily with the lipids in the bilayer region. If the annulus is narrow, it means that there is less interaction between the lipids in the bilayer and the oil molecules.

Figure 2A and 2B show the SH response at the edge of the Teflon film comparing hexadecane (A, green) and squalene (B, red). The width of the annulus of the bilayer is defined as the width of region II in Fig. 1E. Figure 2C shows the width of the annulus for hexadecane and squalene summarizing the results of several membranes (6 and 12 different bilayers respectively). It can be seen that squalene laterally extends further to the bilayer compared to hexadecane.

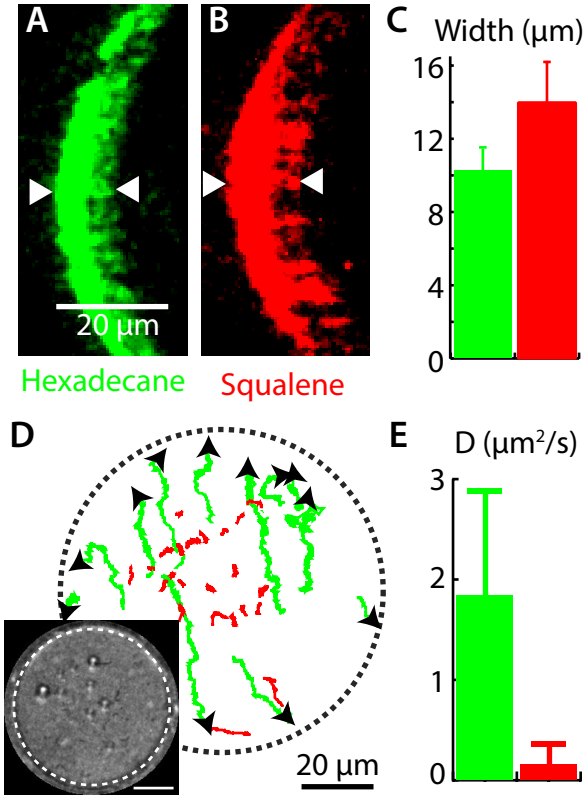

Figure 2. Second harmonic (SH) and white-light imaging of oil and lipid interactions comparing hexadecane and squalene. SH images of bilayers at the edge of the Teflon film (region II in Fig. 1E) for a symmetric neutral membrane composed of DOPC prepared with (**A**) hexadecane and (**B**) squalene. (**C**) The width of the annulus is quantified by the distance between the white arrows as shown in A and B. Squalene has wider width and thus laterally extends further to the bilayer (see the S2 for line profiles). **(D)** Selected white-light tracks of trapped oil micro-lenses showing the directional diffusion of hexadecane (green) and random diffusion of squalene (red). The black arrows indicate the direction of movement. The inset shows a typical white-light image of trapped oil micro-lenses that appear as bright spots. Scale bar is 20 μm and the dashed circles indicate the Teflon edge. **(E)** Calculated diffusion coefficients from the mean square displacement curves (see SI S3 for more details) comparing squalene and hexadecane. Squalene diffuses an order of magnitude slower than hexadecane.

When bilayers are formed they are typically left to equilibrate for several minutes[15-16] while the capacitance increases until it levels off. This is interpreted as thinning of the bilayer. In what follows, we investigate this equilibration process for hexadecane and squalene using white-light imaging. Directly after formation of the bilayer, the white light images display spherical structures or micro-lenses (see inset in Fig. 2D), which also appear in SH images. In the time span of minutes these structures redistribute across the images. We follow these structures and obtain tracks shown in Fig. 2D. The black arrows point to the direction to which the micro-lenses move. It can be seen that hexadecane (green) moves directionally to the edge of the membrane (see the arrows), while squalene (red) stays in the center and moves randomly. Figure 2E displays the calculated diffusion coefficients for several tracks (N=31 for squalene and N=15 for hexadecane, see the SI (S3) for mean

square displacement curves). The mean diffusion coefficient for hexadecane is 1.8 ± 1.0 $\mu m^2/s$, and for squalene is 0.16 ± 0.24 $\mu m^2/s$. Thus, hexadecane droplets diffuse an order of magnitude faster than squalene. These numbers suggest that for a 100-μm diameter membrane, a hexadecane droplet needs ~ 10^2 seconds to leave the center of the bilayer and move to the reservoir at the edge (assuming directional movement). In contrast, with the random movement of squalene ~ 10^4 seconds are required for squalene droplets to cover the whole membrane area and accidentally meet the edge. Therefore, squalene could be trapped within the bilayer for the duration of a typical experiment (1-3 hours) while hexadecane has a higher propensity to move to the edge on the timescale of a few minutes.

Concerning the observed difference in the diffusion coefficients of the oil droplets, the propensity of squalene to diffuse slowly is likely linked to its structure. There are two possible main orientations for the oil: (i) parallel to the membrane, i.e., the oil molecules are primarily situated between the bilayer leaflets, Fig. 3A, or (ii) perpendicular to the membrane, i.e., the oil molecules are oriented parallel with respect to the lipids acyl chains and are either localized within a single leaflet or in both leaflets, Fig. 3B. There are several important structural differences between squalene and hexadecane. Squalene, with 30 C atoms is larger than hexadecane, with 16 C atoms. Squalene is thus also larger than the lipid acyl chains, while hexadecane has the same size. Furthermore, the presence of double bonds in squalene leads to a stiff comb-like molecular conformation. Such a structure facilitates anchoring of squalene to the hydrophobic core. In contrast, the cylindrical structure of hexadecane does not provide this kind of molecular friction and can be more easily expelled to the oil reservoir at the edges. Both differences will ensure larger molecular friction with the acyl tails for squalene than for hexadecane.

To gain more insight into the oil – lipid interactions, we can compare our diffusion values to the diffusion of single lipids and lipid domains that has been measured by fluorescence imaging. Single lipid diffusion was measured using fluorescence correlation spectroscopy (FCS)[32] and fluorescence recovery after photobleaching (FRAP)[33] and is in the order of 10^0 - 10^1 $\mu m^2/s$. Diffusion of liquid-ordered domains in a bilayer on the other hand is in the order of 10^{-3} – 10^{-1} $\mu m^2/s$[34]. The diffusion coefficients found for hexadecane (1.8 ± 1.0 $\mu m^2/s$,) agrees with those found for single lipid diffusion, while the diffusion coefficients found for squalene (0.16 ± 0.24 $\mu m^2/s$) falls in the range of lipid domain diffusion. This agreement suggests that hexadecane diffuses in a similar manner as lipids in a single leaflet, which would mean that hexadecane is oriented perpendicular to the membrane and located primarily within a single leaflet. Squalene on the contrary moves much slower, which, agrees with a squalene induced coupling between the leaflets which could come about either by being oriented perpendicular to the acyl chains of the lipids (Fig. 3) or by being oriented parallel to the lipid acyl chains but spanning over both leaflets. Since the

capacitance values allow a range of thicknesses they are inconclusive regarding the orientation of the oil molecules. Therefore, further investigations are required to confirm these mechanisms (for example by polarized Raman TIR spectroscopy[35] or sum frequency generation[36]).

Experiments in Ref.[27] showed that free standing membranes formed with heptadecane have the highest specific capacitance compared to bilayers formed with other alkanes. Similar conclusions were drawn from experiments on droplet interface bilayers in Refs.[22, 37] suggesting that longer alkyl chains due to their cylindrical structure (but still fitting within one leaflet) should generate more ideal bilayers. To test this hypothesis, we formed freestanding membranes using heptadecane and obtained white light images immediately after membrane formation (thus, before the equilibrated stage investigated in Figs. 1 and 2A-2B). Figure 3C shows the white-light image for a bilayer prepared with heptadecane ~5 s after membrane formation. In comparison, Fig. 3D shows the white-light image for a bilayer prepared with hexadecane ~5 s after membrane formation. We observe that the amount of oil at the edge of the Teflon film is markedly wider for heptadecane directly after membrane formation than for hexadecane, suggesting that immediately after membrane formation, most of the oil is already squeezed out. Waiting longer, ~ 15 mins after membrane formation, Figs. 3E and 3F show the corresponding white light image for heptadecane and hexadecane. We observed in Figs. 3E and 3F that the thickness of the oil at the edge increases for hexadecane but not for heptadecane.

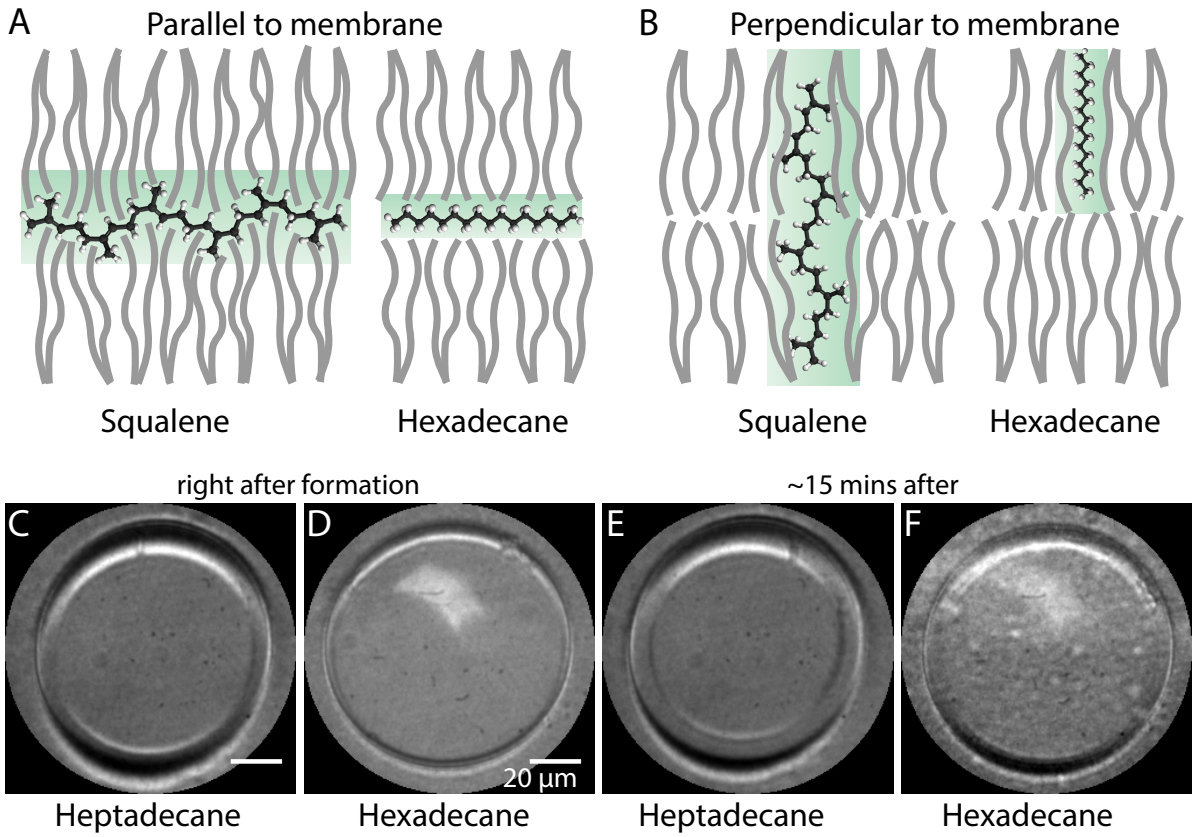

Figure 3. Possible mechanisms for the interaction of oil inside a lipid bilayer. Illustration of the proposed mechanism that explains the observed difference in diffusion when: oil is oriented parallel to the membrane plane **(A)** and oil is oriented perpendicular to the membrane **(B)**. Interdigitating oil with acyl chains is easier for squalene (A, left) than for hexadecane (A, right). The larger size of squalene can span the bilayer leaflets (B, left) compared to hexadecane. The molecular friction for squalene is larger compared to hexadecane thus retarding its diffusion. White-light images of freestanding membranes immediately after formation (**C,D)** and ~15 minutes after formation **(E,F)** for membranes prepared with hexadecane and heptadecane**.** The amount of oil near the Teflon edge immediately after formation for membranes prepared with heptadecane is wider compared to membranes prepared with hexadecane. The scale bar is the same for all images. The Teflon edge is visible and the white light is positioned obliquely coming from the top. The bright shape in the bilayer center in (D, F) is the reflection from the lamp.

The above findings suggest that in order to use a freestanding bilayer system that is completely free of oil, the best chance to reach such a state is by using heptadecane as oil. The disadvantage of using heptadecane is the melting point, T_m = 23 °C, thus requiring temperature control. The practical approach is to use hexadecane (T_m = 18 °C) and wait long enough for oil to be squeezed out. In addition, from a biochemical-interactions perspective, as every living cell contains lipid droplets that are composed of an oily interior (with cholesterol, triglycerides, cholesterol esters and unsaturated fatty acids) covered with a lipid monolayer.[1-2, 4, 38-39] These droplets move freely through the cytoplasm and can merge with the various membranes in the cell. They can be formed by budding-off from a membrane. Although cell membranes are far more complex than the free standing

membrane model studied here, and the oil structures are only comparable but not identical, the found information about the interaction of oil and lipids provides insight into the state of oil inside lipid bilayers, which is useful for understanding the same type of interactions in biological systems.

Conclusions

In summary, we investigated the interaction of oil with freestanding lipid bilayers in aqueous solution using second harmonic and white-light imaging. We find that even on equally high capacitance lipid membranes that are prepared with squalene and hexadecane there are differences in the membrane structure. From the SH intensity profile and the white-light temporal image stacks we conclude that the curvature of monolayers at the edge of the Teflon film of freestanding bilayers prepared with hexadecane is higher compared with squalene, indicating that less hexadecane is present within the bilayer. Conversely it seems there is a higher quantity of squalene remaining in the bilayer since squalene forms a wider annulus. The diffusion tracks show directed diffusion of hexadecane droplets after membrane formation, with a diffusion coefficient of 1.8 $\mu m^2/s$ (i. e. around 10^2 seconds the oil droplets have been expelled to the Teflon edge), while squalene shows no directed motion, with a diffusion coefficient of 0.16 $\mu m^2/s$. There is a similarity with single lipid diffusion (hexadecane) and lipid domain diffusion (squalene). This difference is caused by the difference in structure: hexadecane can stay within a single leaflet and diffuse through the liquid phase of the lipids. Squalene on the other hand is bigger than a single leaflet and also more branched so it will couple to both leaflets and move slower. These differences and the related interaction mechanisms are important when considering what type of bilayer system needs to be used. They may also influence membrane properties in biological systems.

Acknowledgements

This work is supported by the Julia Jacobi Foundation, the European Research Council grant 616305, and the European Union's Horizon 2020 research and innovation program under Marie Skłodowska-Curie grant agreement 721766 (FBI).

Supplementary Information

The supplementary information contains information about: (S1) sample preparation and instrumentation, (S2) measurement of the width of the annulus, (S3) diffusion of oil droplets for bilayers prepared with hexadecane and squalene.

References

1. Thiam, A. R.; Farese, R. V.; Walther, T. C., The Biophysics and Cell Biology of Lipid Droplets. *Nature reviews. Molecular cell biology* **2013,** *14* (12), 775-786.
2. Gao, Q.; Goodman, J. M., The lipid droplet—a well-connected organelle. *Frontiers in Cell and Developmental Biology* **2015,** *3*, 49.
3. Brasaemle, D. L., The perilipin family of structural lipid droplet proteins: Stabilization of lipid droplets and control of lipolysis. *Journal of Lipid Research* **2007**.
4. Goodman, J. M., The Gregarious Lipid Droplet. *The Journal of Biological Chemistry* **2008,** *283* (42), 28005-28009.
5. Kessel, A.; Cafiso, D. S.; Ben-Tal, N., Continuum Solvent Model Calculations of Alamethicin-Membrane Interactions: Thermodynamic Aspects. *Biophysical Journal* **2000,** *78* (2), 571-583.
6. Marsh, D.; Jost, M.; Peggion, C.; Toniolo, C., Lipid Chain-Length Dependence for Incorporation of Alamethicin in Membranes: Electron Paramagnetic Resonance Studies on TOAC-Spin Labeled Analogs. *Biophysical Journal* **2007,** *92* (11), 4002-4011.
7. Binder, W. H.; Barragan, V.; Menger, F. M., Domains and Rafts in Lipid Membranes. *Angew. Chem., Int. Ed.* **2003,** *42* (47), 5802-5827.
8. Cicuta, P.; Keller, S. L.; Veatch, S. L., Diffusion of Liquid Domains in Lipid Bilayer Membranes. *The Journal of Physical Chemistry B* **2007,** *111* (13), 3328-3331.
9. Alvarez, O.; Latorre, R., Voltage-dependent capacitance in lipid bilayers made from monolayers. *Biophysical journal* **1978,** *21* (1), 1-17.
10. Lütgebaucks, C.; Macias-Romero, C.; Roke, S., Characterization of the interface of binary mixed DOPC:DOPS liposomes in water: The impact of charge condensation. *The Journal of Chemical Physics* **2017,** *146* (4), 044701.
11. Smolentsev, N.; Lütgebaucks, C.; Okur, H. I.; de Beer, A. G. F.; Roke, S., Intermolecular Headgroup Interaction and Hydration as Driving Forces for Lipid Transmembrane Asymmetry. *Journal of the American Chemical Society* **2016,** *138* (12), 4053-4060.
12. Ho, J. C. S.; Rangamani, P.; Liedberg, B.; Parikh, A. N., Mixing Water, Transducing Energy, and Shaping Membranes: Autonomously Self-Regulating Giant Vesicles. *Langmuir* **2016,** *32* (9), 2151-2163.
13. Richter, R. P.; Berat, R.; A Brisson, A., Formation of solid-supported lipid bilayers: An integrated view. *Langmuir* **2006,** *22* (8), 3497-3505.
14. Angelova, M. I.; Soléau, S.; Méléard, P.; Faucon, F.; Bothorel, P., *Preparation of giant vesicles by external AC electric fields. Kinetics and applications*. Steinkopff: Darmstadt, 1992; p 127-131.
15. White, S. H.; Petersen, D. C.; Simon, S.; Yafuso, M., Formation of planar bilayer membranes from lipid monolayers. A critique. *Biophysical journal* **1976,** *16* (5), 481-489.
16. Montal, M.; Mueller, P., Formation of bimolecular membranes from lipid monolayers and a study of their electrical properties. *Proceedings of the National Academy of Sciences of the United States of America* **1972,** *69* (12), 3561-3566.
17. Collins, M. D.; Keller, S. L., Tuning lipid mixtures to induce or suppress domain formation across leaflets of unsupported asymmetric bilayers. *Proceedings of the National Academy of Sciences* **2008,** *105* (1), 124-128.
18. Veatch, S. L.; Polozov, I. V.; Gawrisch, K.; Keller, S. L., Liquid domains in vesicles investigated by NMR and fluorescence microscopy. *Biophysical journal* **2004,** *86* (5), 2910-2922.
19. Veatch, S. L.; Keller, S. L., Seeing spots: Complex phase behavior in simple membranes. *Biochimica et Biophysica Acta (BBA) - Molecular Cell Research* **2005,** *1746* (3), 172-185.
20. Bakht, O.; Pathak, P.; London, E., Effect of the structure of lipids favoring disordered domain formation on the stability of cholesterol-containing ordered domains (lipid rafts): identification of multiple raft-stabilization mechanisms. *Biophys J* **2007,** *93* (12), 4307-18.
21. Dietrich, C.; Bagatolli, L. a.; Volovyk, Z. N.; Thompson, N. L.; Levi, M.; Jacobson, K.; Gratton, E., Lipid rafts reconstituted in model membranes. *Biophysical journal* **2001,** *80* (3), 1417-1428.
22. Gomopoulos, N.; Lütgebaucks, C.; Sun, Q.; Macias-Romero, C.; Roke, S., Label-free second harmonic and hyper Rayleigh scattering with high efficiency. *Optics Express* **2013,** *21* (1), 815-821.

23. Gutsmann, T.; Heimburg, T.; Keyser, U.; Mahendran, K. R.; Winterhalter, M., Protein reconstitution into freestanding planar lipid membranes for electrophysiological characterization. *Nature Protocols* **2014,** *10* (1), 188-198.
24. Macias-Romero, C.; Didier, M. E. P.; Jourdain, P.; Marquet, P.; Magistretti, P.; Tarun, O. B.; Zubkovs, V.; Radenovic, A.; Roke, S., High throughput second harmonic imaging for label-free biological applications. *Optics express* **2014,** *22* (25), 31102-12.
25. Tarun, O. B.; Hannesschläger, C.; Pohl, P.; Roke, S., Label-free and charge-sensitive dynamic imaging of lipid membrane hydration on millisecond time scales. *Proceedings of the National Academy of Sciences* **2018,** *115* (16), 4081.
26. Macias-Romero, C.; Didier, M. E. P.; Zubkovs, V.; Delannoy, L.; Dutto, F.; Radenovic, A.; Roke, S., Probing rotational and translational diffusion of nanodoublers in living cells on microsecond time scales. *Nano letters* **2014,** *14* (5), 2552-7.
27. White, S. H., Studies of the physical chemistry of planar bilayer membranes using high precision measurements of specific capacitance. *Annals of the New York Academy of Sciences* **1977,** *303*, 243-265.
28. Benz, R.; Fröhlich, O.; Läuger, P.; Montal, M., Electrical capacity of black lipid films and of lipid bilayers made from monolayers. *Biochimica et Biophysica Acta (BBA) - Biomembranes* **1975,** *394* (3), 323-334.
29. White, S. H., Ion channel reconstitution. *Ion Channel Reconstitution* **1986**, 3-34.
30. Israelachvili, J. N., *Intermolecular and Surface Forces. 3rd edition*. Elsevier: 2011.
31. Boyd, R. W., *Nonlinear Optics, Third Edition*. Academic Press: 2008.
32. Horner, A.; Akimov, S. A.; Pohl, P., Long and Short Lipid Molecules Experience the Same Interleaflet Drag in Lipid Bilayers. *Physical Review Letters* **2013,** *110* (26).
33. Almeida, P. F.; Vaz, W. L.; Thomson, T. E., Lateral Diffusion in the Liquid Phases of Dimyristoylphosphatidylcholine/Cholesterol Lipid Bilayers: A Free Volume Analysis. *Biochemistry* **1992,** *32*, 6739-6747.
34. Cicuta, P.; Keller, S. L.; Veatch, S. L., Diffusion of liquid domains in lipid bilayer membranes. *Journal of Physical Chemistry B* **2007,** *111* (13), 3328-3331.
35. Tyrode, E.; Rutland, M. W.; Bain, C. D., Adsorption of CTAB on Hydrophilic Silica Studied by Linear and Nonlinear Optical Spectroscopy. *Journal of the American Chemical Society* **2008,** *130* (51), 17434-17445.
36. Roke, S., Nonlinear Optical Spectroscopy of Soft Matter Interfaces. *Chemphyschem* **2009,** *10* (9-10), 1380-1388.
37. Horner, A.; Siligan, C.; Cornean, A.; Pohl, P., Positively charged residues at the channel mouth boost single-file water flow. *Faraday Discuss.* **2018**.
38. Boström, P.; Andersson, L.; Rutberg, M.; Perman, J.; Lidberg, U.; Johansson, B. R.; Fernandez-Rodriguez, J.; Ericson, J.; Nilsson, T.; Borén, J.; Olofsson, S.-O., SNARE proteins mediate fusion between cytosolic lipid droplets and are implicated in insulin sensitivity. *Nature Cell Biology* **2007,** *9*, 1286.
39. Spanova, M.; Zweytick, D.; Lohner, K.; Klug, L.; Leitner, E.; Hermetter, A.; Daum, G., Influence of squalene on lipid particle/droplet and membrane organization in the yeast Saccharomyces cerevisiae. *Biochimica et Biophysica Acta* **2012,** *1821* (4), 647-653.